Comparative analysis of interactions of RASSF1-10

Jia Jia Chan[a], Delphine Flatters[b], Fernando Rodrigues-Lima[c], Jun Yan[a], Konstantinos Thalassinos[a], Matilda Katan[a,]*

[a] Institute of Structural and Molecular Biology, Division of Biosciences, University College London, Gower Street, London WC1E 6BT, UK

[b] Université Paris Diderot, Sorbonne Paris Cité, Molécules Thérapeutiques in silico, Inserm UMR-S 973, 35 rue Helene Brion, 75013 Paris, France

[c] Université Paris Diderot, Sorbonne Paris Cité, Unité de Biologie Fonctionnelle et Adaptative, CNRS EAC4413, 75013, Paris, France

*Corresponding author. Darwin Building, University College London, Gower Street, London WC1E 6BT, UK; e-mail address: m.katan@ucl.ac.uk

Abstract

Members of the RASSF family (RASSF1-10) have been identified as candidate tumour suppressors that are frequently downregulated by promoter hypermethylation in cancers. These proteins carry a common Ras-association (RA) and SARAH domain (RASSF1-6) that can potentially bind Ras oncoproteins and mediate protein-protein interactions with other SARAH domain proteins. However, there is a notable lack of comparative characterisation of the RASSF family, as well as molecular and structural information that facilitate their tumour suppressive functions. As part of our comparative analysis, we modelled the RA and SARAH domains of the RASSF members based on existing structures and predicted their potential interactions. These *in silico* predictions were compared to *in vitro* interaction studies with Ras and MST kinase (a SARAH domain-containing protein). Our data shows a diversity of interaction within the RASSF family RA domain, whereas the SARAH domain-mediated interactions for RASSF1-6 are consistent with the predictions. This suggests that different members, despite shared general architecture, could have distinct functional properties. Additionally, we identify a new interacting partner for MST kinase in the form of RASSF7. Current data supports an interaction model where RASSF serves as an adaptor for the assembly of multiple protein complexes and further functional interactions, involving MST kinases and other SARAH domain proteins, which could be regulated by Ras.

Keywords

RASSF, MST, RA, SARAH, Ras

Introduction

The Ras-association domain family (RASSF) comprises of 10 members, known as RASSF1 to RASSF10. The RASSF proteins carry several characteristic domains and function as adaptor proteins in many important biological processes, such as pro-apoptotic pathways, cell cycle and cytoskeleton regulation. Studies have also shown that expression of many RASSF members is downregulated by promoter hypermethylation in various types of cancers, including colorectal, lung, breast, prostate and brain cancers (Akino et al., 2005; Dammann et al., 2000; Eckfeld et al., 2004). This epigenetic silencing of RASSF1 has also been linked to advanced tumour stage and poor prognosis (Pfeifer and Dammann, 2005). However, in many cases, over-expression or re-expression leads to cell cycle arrest or growth suppression (Burbee et al., 2001; Eckfeld et al., 2004; Ikeda et al., 2007; Vos et al., 2003b). When presented together, these characteristics make the RASSF family potential cancer markers and tumour suppressors.

The ten RASSF members are divided into two sub-categories: the classical RASSFs (RASSF1-6) and N-terminal RASSFs (RASSF7-10) (Fig. 1). All members carry a common Ras-association (RA) domain. As the Ras genes are mutated in 20 to 25% of human tumours (Downward, 2003), the RA domain and its ability to interact with various Ras GTPases carry particular importance in the RASSF tumour suppressor function. Despite this, only the RA domain for RASSF5 has been characterised by X-ray crystallography (Stieglitz et al., 2008). It displays the conserved ubiquitin-fold and binds to HRas with a sub-micromolar affinity; however, its doubly large size of 160 residues sets it apart from other well characterised RA domains, such as that of RalGDS, c-Raf and PLCε (Bunney et al., 2006; Huang et al., 1998; Nassar et al., 1996), due to an N-terminal subdomain required to make contact with the Ras switch II interface. The high homology amongst RASSF1-6 suggests similar structural arrangement and behaviour for these potential Ras effectors. There have been numerous studies showing different classical RASSF members binding to various Ras GTPases (Dallol et al., 2009; Miertzschke et al., 2007; Rodriguez-Viciana et al., 2004; Stieglitz et al., 2008; Vos et al., 2000). However, several of these reports are contradictory (Richter et al., 2009; Rodriguez-Viciana et al., 2004). Information regarding the RA domain for the N-terminal RASSFs is even scarcer, with only two reports of Ras binding by RASSF7 and RASSF9 (Rodriguez-Viciana et al., 2004; Takahashi et al., 2011).

Much of the RASSF function in the pro-apoptotic pathway involves the Sav/RASSF/Hippo (SARAH) domain (Fig. 1) and its ability to mediate protein-protein interactions. The SARAH domain has been shown to facilitate dimerisation between SARAH domain-containing proteins, which allows all the classical RASSF members to interact with a family of pro-apoptotic kinases, known as the Mammalian sterile 20-like (MST) kinases (Cooper et al., 2008; Hwang et al., 2007; Ikeda et al., 2009;

Khokhlatchev et al., 2002; Praskova et al., 2004). The only known structure of the SARAH domain comes from MST1 kinase. It consists of two α-helices and forms homodimers or heterodimers with RASSF5 via two anti-parallel α-helices (Hwang et al., 2007). It was also reported that the SARAH domain has a higher propensity for forming heterodimers compared to homodimers; and more recently, this dimerisation helps to stabilise the SARAH domain structure (Constantinescu Aruxandei et al., 2011). The ability to oligomerise is crucial for the functions of both MST1 kinase and RASSF, the latter of which was shown to enhance MST1 activity to promote apoptosis upon Ras-binding (Avruch et al., 2006). The SARAH domain is not present in the N-terminal RASSFs; however, an alternative coiled-coil structure has been predicted at the C-terminal region of RASSF7, RASSF8 and RASSF10. This could potentially function similarly to the SARAH domain, although there is no evidence as yet of interaction mediated by the coiled-coil motif.

Despite numerous studies on the RASSF family in recent years and the increasing evidence highlighting their role as potential tumour suppressors, most RASSF members remain poorly characterised. There is a notable lack of in-depth, comparative characterisation of the RASSF family at the molecular level; information on structure and underlying molecular mechanisms that facilitate the RASSF tumour suppressive functions is also scarce. Here, we present a comprehensive comparative analysis of the RA and SARAH domains of all the RASSF family members using both *in silico* predictions and *in vitro* experimentations.

Materials and Methods

Cloning, Protein Expression and Purification

Constructs used for bacterial cell expression were prepared in pTriEx4 (Novagen) as outlined (Bunney et al., 2006). The following constructs used in this study were described previously: pTriEx4 RAPL (RASSF5) SARAH (residues 212-265) (Miertzschke et al., 2007) and HRas G12V (Bunney et al., 2006). All constructs above and MST1 SARAHmyc (residues 432-487) were expressed in *E. coli* and purified as described (Miertzschke et al., 2007). For interaction studies, MST1 (residues 1-487), MST2 (residues 1-491) and their kinase-dead mutants MST1 K59R and MST2 K56R were cloned into pTriEx6 (Novagen) with an additional myc tag. Other constructs used were cloned into pEGFP-C1 (Clontech) and pTagRFPT-C1, which were converted to Gateway compatible vectors. pTagRFPT-C1 was derived from pEGFP-C1 by swapping the fluorophores using restriction digests and ligation at the NheI and BglII sites. All RASSF5 constructs used in this study were derived from the RASSF5C isoform, which is identical to RASSF5A in the RA and SARAH domain regions. All mutagenesis was carried out using the QuickChange Site-Directed Mutagenesis Kit (Stratagene), following the manufacturer's instructions. All constructs were verified by sequencing.

Protein Modelling

The sequences encoding the RA domain and SARAH domain were predicted using PROSITE. For RASSF1-4 and RASSF6, the RA domain sequences were aligned to the template of RASSF5 (NORE1) RA domain (PDB: 3DDC) excluding the N-terminal subdomain (residues 274-358). The sequences of the predicted RA domain for RASSF7-9 were aligned to c-RAF RBD (PDB: 1GUA). All RA domain alignments were performed and 3D models generated and evaluated as described (Miertzschke et al., 2007). The SARAH domains of RASSF1-6 were aligned to the template of MST1 kinase SARAH (PDB: 2JO8) using Prosite multiple sequence alignment. The 3D models were constructed using Modeller v9.8 (Eswar et al., 2006). 100 dimer models were calculated and the chosen model for each RASSF represents the best model with the lowest objective function. RASSF7 coiled-coil models were constructed *de novo* using Quark online server (available on World Wide Web) (Xu and Zhang, 2012). The models were evaluated and validated using the same method as above.

In vitro Pull-Down Assays

The *in vitro* pull-down assays were carried out as described by Miertzschke et al. (2007) with a few minor adjustments. Full length RASSFs, which could not be purified, were each expressed in 30ml Freestyle 293F cell cultures as described (Bunney et al., 2012), but in a linearly scaled-down system. Each culture was transfected with 37.5µg of pEGFP-C1 RASSF construct. Cells were harvested after 72 hours and lysed in modified Nonidet P-40 lysis buffer (0.1% Nonidet, 25mM Tris-HCl pH7.5,

150mM NaCl, protease inhibitor) for 15 minutes at 4°C. The cell lysates were incubated with immobilised S-tagged small GTPases loaded with nucleotide for 1 hour at 4°C with constant agitation and washed three times with Nonidet P-40 buffer. For pull-down assays of SARAH domain proteins, 50µg of immobilised S-tagged RASSF5 SARAH was incubated with 50µg MST1 SARAHmyc for 1 hour with constant agitation. The beads were washed three times with phosphate-buffered saline. Protein-protein interactions were analysed by SDS-PAGE stained with Coomassie blue or by Western blotting with anti-GFP (B2) antibody (Santa Cruz).

Co-immunoprecipitation (Co-IP)

293F cells were co-transfected with different DNA constructs (19µg/ construct) in 30ml cultures and lysed after 72 hours in CellLytic M Cell Lysis Reagent (Sigma). The cell lysates were incubated with anti-c-myc agarose affinity gel antibody (Sigma) for 1 hour at 4°C with constant agitation and washed five times with phosphate-buffered saline. Protein-protein interactions were analyzed by Western blotting with anti-GFP (B2) (Santa Cruz), anti-tRFP (Evrogen) and anti-myc (in-house) antibodies.

Mass Spectrometry (MS)

Mass spectrometry experiments were carried out on a first-generation Synapt HDMS (Waters Corp., Manchester, UK) Quadrupole-TOF mass spectrometer (Pringle et al., 2007). Samples were buffer exchanged into 150mM ammonium acetate using Biospin-6 columns (Bio-Rad). For the mixing experiment, equal-molar of MST1 SARAHmyc and RASSF5 SARAH were incubated for 1 hour at 4°C prior to MS analysis. 2.5µl aliquots of the protein sample of 15µM in concentration were introduced to the mass spectrometer by means of nano-electrospray ionisation using gold-coated capillaries prepared in-house. The instrument was mass calibrated using a 33µM solution of Cesium Iodide in 250mM ammonium acetate. Typical instrumental parameters were as follows: capillary voltage 1.0 kV, cone voltage 50 V, trap energy 6 V, transfer energy 4 V, bias voltage 2.0 V, and trap pressure 8.6e^-3 mbar.

Results and Discussion

RA domain and its interaction with Ras GTPases

Modelling the RASSF RA domain and predicting its interactions

Several approaches have been used to model protein domains in order predict new protein interactions. Kiel et al. (2007) used a sophisticated method involving various protein design algorithms to draw network interactions between different Ras GTPases and putative Ras-binding domains (RBDs). There is no structural distinction between RA and RBD, which are only different names used for the same ubiquitin fold. The same study also highlighted the significance of amino acid conservation on the protein surface in determining interaction. As general electrostatic interactions are important in Ras/ RA binding due to the highly negatively charged surface on the Ras switch I and II regions (Kiel et al., 2004; Nassar et al., 1996), an overall positive charge of the RA domain surface would suggest that one of the key criteria for Ras binding is fulfilled. However, as also shown by structurally characterised RA or RBD domains, such as RASSF5, RalGDS, c-Raf and PLCε (Bunney et al., 2006; Huang et al., 1998; Nassar et al., 1996; Stieglitz et al., 2008), residues directly involved in interactions with Ras switch I and II regions are difficult to predict.

In order to further understand the RA domain of the remaining RASSF members and its potential interactions with Ras GTPases, we employed a simpler approached previously used by Miertzschke et al. (2007) to model their RA domain against templates of structurally known RA domain (Fig. 2). We first performed a sequence alignment of the classical RASSF members RA domain with the only structurally known RASSF RA domain, RASSF5 (Fig. 2A). Only the RA domain sequences predicted by Prosite were used for alignments and modelling, which excludes the N-terminal subdomain and β1 strand of the RASSF5 template. The main residues involved in electrostatic interactions are found in β2 and the C-terminus of α1. Several key residues, such as P278, K303 and F304 are highly conserved. However, other important residues in β2 aligning to D280, I281, K282 and Q283 are not as well conserved, with RASSF1 sharing the most conserved residues with RASSF5.

For each RASSF model, the alignments were manually adjusted to obtain the optimal fit. Due to the exclusions we made to the template, β2 in our models, including the remodelled RASSF5 template (Supplementary Fig. 1A), is not seen as a strand due to its anti-parallel position with β1 in the original RASSF5 template. In the RASSF2, RASSF4 and RASSF6 models, β4 is also missing due to the gap aligning to that region (Fig. 2A). Despite several differences in the key interacting residues, there are no major changes in the electrostatic surface for all models in the regions of β2 and α1, with the exception of RASSF3, which appears to have a neutral surface around the β2 region (Fig. 2B). However, theoretically, these changes should not affect Ras interaction of most of the classical RASSF members as they are not within the interacting surfaces.

A different RBD, c-Raf RBD, was used as a modelling template for the N-terminal RASSF members. Fig. 2C shows good alignment between c-Raf and RASSF7 and RASSF8 where most key interacting residues in β1 and β2, such as R59, Q66, R67 and V69, are conserved. RASSF9 RA domain amino acid residues are not as well conserved in comparison, with only a conserved and a semi-conserved residue at the positions of V69 and R67. Unlike the classical RASSF members, the residues aligning to the α1 region are not well conserved.

These differences observed in the alignments are evident in the three dimensional models (Fig. 2D). For RASSF7 and RASSF8, there are no major electrostatic surface changes in the β1 and β2 regions. However, the α1 region, which is highly positively charged in c-Raf (Supplementary Fig. 1B), is now neutral. This change is more significant for RASSF9, where the β2 region appears more negatively charged. The electrostatic potential changes observed in RASSF7 and RASSF8 may not completely eliminate their ability to interact with Ras, but may serve to weaken this interaction.

Overall, the models suggest a high possibility of Ras interaction for all the classical RASSF members apart from RASSF3, and two N-terminal RASSF members RASSF7 and RASSF8. Whereas the reversal of electrostatic potential in the main interaction surfaces of RASSF9 suggests a non-binder. The RA domain of RASSF10 could not be properly aligned and modelled against any known RA domain, thus, its Ras interaction could only be determined experimentally.

RA domain of RASSF1-10 shows differential Ras interactions

Apart from RASSF5, several studies have reported the interaction of different classical RASSF members with various Ras GTPases and even Ran GTPase. However, many of the *in vitro* interactions observed are ambiguous and the methods used to show interaction were widely different.

In order to test the *in silico* predictions and determine whether the predicted RASSF RA domains are able to bind Ras, we performed an *in vitro* pull-down for the whole panel of RASSF family using activated HRas G12V. RASSF5 essentially served as a positive control. We show GTP-dependent binding to HRas by RASSF3, RASSF4 and RASSF6 from the classical subgroup and RASSF7 from the N-terminal subgroup (Fig. 3A). It should be noted that the pull-down method used in this study typically detects binding affinities of up to a dissociation constant (k_D) of 10μM (Bunney et al., 2006). Protein interactions with a high k_D (weak binding) or fast off rates (k_{off}) will be impossible to detect using such method.

These observations demonstrate that surface electrostatic potential predictions are informative and true to a certain extent but insufficient to determine definite interactions. This is evident when the *in*

silico predictions are compared to the *in vitro* results. RASSF1, which interaction surface and residues most resemble RASSF5, and RASSF2, which also has a similar surface potential, did not interact with HRas or KRas G12V (not shown). In addition, despite both having a similar positively charged surface, RASSF4 proved to be a much weaker binder compared to RASSF6. They also showed differential binding to KRas (data not shown): weak binding for RASSF4 and no binding for RASSF6. Conversely, RASSF3, which shared minimal conserved residues with RASSF5 and had a more neutral binding interface, was the unexpected binder to both HRas and KRas, albeit a weak one (data not shown).

The predictions for the N-terminal RASSF members appear slightly more accurate. The GTP-dependent binding of RASSF7 to HRas, KRas and NRas (data not shown) is in agreement with a recent report of NRas interaction (Takahashi et al., 2011). Also true to prediction is RASSF9, which had a negatively charged surface, thus did not show any binding. However, it is also puzzling that RASSF8, which displays almost identical surface potential and conserved residues to RASSF7, did not bind any GTPases.

RASSF5 and RASSF7 are to be the most consistent Ras binders compared to the remaining RASSF members. Comparison of our data with existing reports suggests the RA domain may have different affinities for different Ras GTPases, such as the reported specificity of RASSF1 for Ran GTPase (Dallol et al., 2009). However, some of our observations are contradictory to previous findings, such as the KRas specificity of RASSF2 (Vos et al., 2003a), RASSF4 (Eckfeld et al., 2004) and RASSF6 (Allen et al., 2007), and the only report to date of Ras interaction by RASSF9 (Rodriguez-Viciana et al., 2004). In addition, a strongly positively charged surface does not always signify a strong binder, as demonstrated by our *in vitro* pull-down. The differences between previous studies and our data could be due to different experimental conditions, Ras specificity, binding affinities and the requirement of a third binding partner, such as that reported by Ortiz-vega et al. (2002), or other regions of the RASSF proteins in addition to the predicted RA domain, such as an equivalent to the N-terminal subdomain in RASSF5 (Stieglitz et al., 2008).

SARAH domain and its ability to mediate oligomerisation

Modelling the RASSF SARAH domain and predicting its interactions

To date, only the SARAH domain from MST1 kinase has been structurally resolved by Hwang et al. (2007). The study demonstrated the significance of hydrophobic interactions mediated by a network of non-polar amino acid residues in facilitating homodimerisation and heterodimerisation as well as maintaining the stability of the dimers. The SARAH domain is found in all six members of the classical RASSF subgroup. However, structural information regarding the RASSF SARAH domain remains scarce despite various reports on heterodimerisation between MST kinase and different

classical RASSF members and the integral role it plays in the biological functions of the RASSF family. The RASSF SARAH domain has never been modelled. It is not known whether the critical residues involved in oligomerisation are present in the SARAH domain of all the classical RASSF members.

In this study, we aligned the RASSF SARAH domain sequences predicted by Prosite with the structurally known MST1 kinase SARAH domain and modelled each RASSF SARAH using these alignments. The sequence alignments show a high level of conservation of most residues involved in maintaining dimer stability (Fig. 4A). Most residues involved in hydrophobic interactions (L444, L451, L448, I459, I462 and Y466) are very well conserved except M455. The two residues involved in electrostatic interaction are D452 and R470; the first is conserved only in RASSF3 and RASSF5, but the latter appears very well conserved. The physico-chemical properties of the residues aligning to those involved in stabilising the H1 and H2 helices in MST1 monomer (L436, W439, V441, L444, I473 and I477) are generally conserved, thus still allowing for hydrophobic interactions.

Dimeric SARAH domain models were constructed for each of the classical RASSF member. Fig. 4B shows the best model out of the 100 dimer models calculated for each RASSF. The distribution of the hydrophobic residues along helix H2 is very similar across all six RASSF members and is also comparable to that of MST1 kinase (Supplementary Fig. 1C). Despite the poor conservation of residues aligning to D452, the models suggest electrostatic interactions with the second helix H2 are still possible due to the presence of a stretch of acidic residues between the regions aligning to L451 and I459. Based on the conservation of the main features involved in dimerisation, we predict that all six classical RASSF members will be able to homodimerise and heterodimerise with MST kinases.

The SARAH domain is notably absent from the N-terminal RASSF members. However, coiled-coil domains have been predicted for RASSF7, RASSF8 and RASSF10 (Fig. 1) and this motif is known to facilitate oligomerisation (Lupas, 1996). As the C-terminus of the SARAH domain also displays relatively high coiled-coil propensity and characteristics (Scheel and Hofmann, 2003), it is possible that the coiled-coils predicted for the N-terminal RASSF members could behave similarly to the SARAH domain and mediate homotypic or heterotypic interactions.

SARAH domain mediates dimerisation between RASSF and MST kinases

Hwang et al. (2007) were the first to elucidate the structure of a SARAH domain and demonstrate homodimerisation of the MST1 kinase SARAH domain as well as its heterodimerisation with RASSF5 in a 1:1 stoichiometry. Various studies have also shown heterodimerisation between MST kinases and RASSF1 (Dittfeld et al., 2012), RASSF2 (Cooper et al., 2009), RASSF5 (Khokhlatchev et al., 2002) and RASSF6, leading to pro-apoptotic effects (Ikeda et al., 2009). Interestingly, RASSF1

was also reported to heterodimerise with RASSF5 to facilitate the tumour suppressor function of the latter (Macheiner et al., 2009). However, these interactions have not been compared across the entire RASSF family to determine whether all the predicted SARAH domains behave similarly.

In the majority of the dimerisation studies using co-expression in cells, we used kinase-dead MST mutants, MST1 K59R and MST2 K56R due to their consistent and higher expression levels. First, we compared RASSF5 dimerisation with wild-type and kinase-dead MST1 and MST2. RASSF5 co-immunoprecipitated equally with all four types of MST kinases tested (Fig. 5A) but the SARAH deletion mutant RASSF5Δ213-265 did not (Fig. 5B). This confirmed that the kinase activity does not interfere with dimerisation and the RASSF SARAH domain is crucial for interaction.

In the following co-immunoprecipitation assay, the complete panel of all ten RASSF members were tested for their interaction with MST1 and MST2. All classical RASSF members co-immunoprecipitated with MST1 (Fig. 5C, left). A similar interaction pattern is observed with MST2, with the exception of RASSF1 (Fig. 5C, right). This varied detection of RASSF1 between the two MST kinases could be due to lower expression levels of RASSF1 and MST2 when co-expressed, rather than a difference in its interaction with MST1 and MST2. We also show, for the first time, interaction between RASSF7 and both MST1 and MST2.

A negative control experiment in which MST was not immunoprecipitated showed negligible precipitation of RASSF5 and RASSF7, which confirmed that the RASSF7 interaction observed was not a false positive (Fig. 5Da). Since the SARAH domain is absent in RASSF7, we looked at its two predicted coiled-coil regions, termed here as coiled-coil 1 and coiled-coil 2. *De novo* protein structure predictions were performed on the two sequences since they do not align well to any known templates. Both regions are predicted to form a single helical structure rich in amino acids with aliphatic side chains (Fig. 5Db), which implies a high probability of a hydrophobic core to facilitate dimerisation.

In addition, we also compared interactions of the isolated SARAH domains *in vitro* and in a cell context. In an *in vitro* pull-down using purified SARAH domain proteins, MST1 SARAHmyc did not interact with immobilised S-RASSF5 SARAH (Supplementary Fig. 2A). We also did not detect any heterodimers when these two proteins were mixed and subjected to mass spectrometry (MS) (Supplementary Fig. 2B, bottom spectrum). However, monomers and homodimers were detected with sizes identical to those for MST1 and RASSF5 SARAH individually (Supplementary Fig. 2B, top, middle spectra and table). In contrast, co-immunoprecipitation analysis shows that the RASSF5 SARAH domain was able to heterodimerise with both full length MST1 and the MST1 SARAH domain in a cell context (Supplementary Fig. 2C).

Our experimental observations match well with the *in silico* predictions of the RASSF SARAH domain interactions. All six classical RASSF members were able to heterodimerise with the MST kinases. Although not tested in this study, there is a high probability of homotypic and heterotypic interactions within the RASSF family itself based on the high accuracy of the models and predictions. The difference observed in heterodimerisation for the isolated SARAH domain between *in vitro* and in cells, with the specific example of RASSF5, suggests a higher natural propensity for the SARAH domain to homodimerise and heterodimerisation may not be preferred in some instances. Furthermore, heterotypic interactions may require specific conditions and factors found in cellular systems or additional interaction sites outside the SARAH domain.

Conclusion

To date, many studies have suggested that Ras-binding and dimerisation of RASSF, mediated by the RA and SARAH domains respectively, facilitate its anti-tumourigenic functions (Richter et al., 2009). However, functional links of RASSF, Ras and other SARAH domain-containing proteins are not clear, with such direct interactions defined only for RASSF5 (Hwang et al., 2007; Stieglitz et al., 2008).

Both *in silico* predictions and *in vitro* experimentations of the RA domain are important in the study of its binding characteristics in different RASSF members. The difficulty in expressing the proteins for the individual RA domains remains a major hurdle in studying the properties of the isolated RA domains. Current data suggests differential binding characteristics for each RA domain despite certain shared conserved residues and architecture. However, negative detection of binding for specific RASSF members in this study should not rule out possible interactions with different Ras GTPases due to a broad range of factors and conditions that could affect such interactions.

The analysis of the SARAH domain was much easier in comparison. This was in part due to good alignments and amino acid residue conservation, hence simpler modelling and predictions. Experimental data supports, and even exceeds our predictions as we identify new interaction pairs between RASSF7 and both MST1 and MST2. However, conditions required for heterodimerisation and the region in RASSF7 that mediates this interaction remain to be further clarified.

Based on our current understanding of the RA and SARAH domains, we propose a model for the assembly of signalling complexes involving the RASSF proteins (Fig. 6). Interactions between the RA domain and members of the Ras GTPase family could result in the translocation of the SARAH domain complexes to the membrane and provide an integrative platform for the assembly of larger complexes and/ or further functional interactions. The consequences of Ras-binding could also involve conformational changes that influence SARAH-mediated dimerisation, consequently the regulation of SARAH-domain proteins, such as the MST kinases.

Further interaction and structural studies will provide a greater understanding on the molecular properties of the RASSF family. These insights will also reinforce our proposed model of interactions and underline the significance of specific protein-protein interactions in driving the potential tumour suppressor properties of RASSF.

Conflict of interest statement

There are no conflicts of interest.

Acknowledgements

This work is supported by Cancer Research UK and Wellcome Trust.

Reference

Akino K, Toyota M, Suzuki H, Mita H, Sasaki Y, Ohe-Toyota M, et al. The Ras Effector RASSF2 Is a Novel Tumor-Suppressor Gene in Human Colorectal Cancer. Gastroenterology 2005;129:156-69.

Allen NP, Donninger H, Vos MD, Eckfeld K, Hesson L, Gordon L, et al. RASSF6 is a novel member of the RASSF family of tumor suppressors. Oncogene 2007;26:6203-11.

Avruch J, Praskova M, Ortiz‐Vega S, Liu M, Zhang XF. Nore1 and RASSF1 Regulation of Cell Proliferation and of the MST1/2 Kinases. Methods Enzymol 2006;407:290-310.

Bunney TD, Esposito D, Mas-Droux C, Lamber E, Baxendale RW, Martins M, et al. Structural and Functional Integration of the PLCgamma Interaction Domains Critical for Regulatory Mechanisms and Signaling Deregulation. Structure 2012.

Bunney TD, Harris R, Gandarillas NL, Josephs MB, Roe SM, Sorli SC, et al. Structural and mechanistic insights into ras association domains of phospholipase C epsilon. Mol Cell 2006;21:495-507.

Burbee DG, Forgacs E, Zöchbauer-Müller S, Shivakumar L, Fong K, Gao B, et al. Epigenetic inactivation of RASSF1A in lung and breast cancers and malignant phenotype suppression. J Natl Cancer Inst 2001;93:691-9.

Constantinescu Aruxandei D, Makbul C, Koturenkiene A, Ludemann MB, Herrmann C. Dimerization-induced folding of MST1 SARAH and the influence of the intrinsically unstructured inhibitory domain: low thermodynamic stability of monomer. Biochemistry 2011;50:10990-1000.

Cooper WN, Dickinson RE, Dallol A, Grigorieva EV, Pavlova TV, Hesson LB, et al. Epigenetic regulation of the ras effector/tumour suppressor RASSF2 in breast and lung cancer. Oncogene 2008;27:1805-11.

Cooper WN, Hesson LB, Matallanas D, Dallol A, von Kriegsheim A, Ward R, et al. RASSF2 associates with and stabilizes the proapoptotic kinase MST2. Oncogene 2009;28:2988-98.

Dallol A, Hesson LB, Matallanas D, Cooper WN, O'Neill E, Maher ER, et al. RAN GTPase is a RASSF1A effector involved in controlling microtubule organization. Curr Biol 2009;19:1227-32.

Dammann R, Li C, Yoon JH, Chin PL, Bates S, Pfeifer GP. Epigenetic inactivation of a RAS association domain family protein from the lung tumour suppressor locus 3p21.3. Nat Genet 2000;25:315-9.

Dittfeld C, Richter AM, Steinmann K, Klagge-Ulonska A, Dammann RH. The SARAH Domain of RASSF1A and Its Tumor Suppressor Function. Mol Biol Int 2012;2012:196715.

Downward J. Targeting RAS signalling pathways in cancer therapy. Nat Rev Cancer 2003;3:11-22.

Eckfeld K, Hesson L, Vos MD, Bieche I, Latif F, Clark GJ. RASSF4/AD037 is a potential ras effector/tumor suppressor of the RASSF family. Cancer Res 2004;64:8688-93.

Eswar N, Webb B, Marti-Renom MA, Madhusudhan MS, Eramian D, Shen MY, et al. Comparative protein structure modeling using Modeller. Curr Protoc Bioinformatics 2006;Chapter 5:Unit 5 6.

Huang L, Hofer F, Martin GS, Kim SH. Structural basis for the interaction of Ras with RalGDS. Nat Struct Biol 1998;5:422-6.

Hwang E, Ryu KS, Paakkonen K, Guntert P, Cheong HK, Lim DS, et al. Structural insight into dimeric interaction of the SARAH domains from Mst1 and RASSF family proteins in the apoptosis pathway. Proc Natl Acad Sci U S A 2007;104:9236-41.

Ikeda M, Hirabayashi S, Fujiwara N, Mori H, Kawata A, Iida J, et al. Ras-association domain family protein 6 induces apoptosis via both caspase-dependent and caspase-independent pathways. Exp Cell Res 2007;313:1484-95.

Ikeda M, Kawata A, Nishikawa M, Tateishi Y, Yamaguchi M, Nakagawa K, et al. Hippo pathway-dependent and -independent roles of RASSF6. Sci Signal 2009;2:ra59.

Khokhlatchev A, Rabizadeh S, Xavier R, Nedwidek M, Chen T, Zhang X-f, et al. Identification of a novel Ras-regulated proapoptotic pathway. Curr Biol 2002;12:253-65.

Kiel C, Foglierini M, Kuemmerer N, Beltrao P, Serrano L. A genome-wide Ras-effector interaction network. J Mol Biol 2007;370:1020-32.

Kiel C, Selzer T, Shaul Y, Schreiber G, Herrmann C. Electrostatically optimized Ras-binding Ral guanine dissociation stimulator mutants increase the rate of association by stabilizing the encounter complex. Proc Natl Acad Sci U S A 2004;101:9223-8.

Lupas A. Coiled coils: new structures and new functions. Trends Biochem Sci 1996;21:375-82.

Macheiner D, Gauglhofer C, Rodgarkia-Dara C, Grusch M, Brachner A, Bichler C, et al. NORE1B is a putative tumor suppressor in hepatocarcinogenesis and may act via RASSF1A. Cancer Res 2009;69:235-42.

Miertzschke M, Stanley P, Bunney TD, Rodrigues-Lima F, Hogg N, Katan M. Characterization of interactions of adapter protein RAPL/Nore1B with RAP GTPases and their role in T cell migration. J Biol Chem 2007;282:30629-42.

Nassar N, Horn G, Herrmann C, Block C, Janknecht R, Wittinghofer A. Ras/Rap effector specificity determined by charge reversal. Nat Struct Biol 1996;3:723-29.

Ortiz-vega S, Khokhlatchev A, Nedwidek M, Zhang X-f, Dammann R, Pfeifer GP, et al. The putative tumor suppressor RASSF1A homodimerizes and heterodimerizes with the Ras-GTP binding protein Nore1. Oncogene 2002;21:1381-90.

Pfeifer GP, Dammann R. Methylation of the tumor suppressor gene RASSF1A in human tumors. Biochemistry 2005;70:576-83.

Praskova M, Khoklatchev A, Ortiz-Vega S, Avruch J. Regulation of the MST1 kinase by autophosphorylation, by the growth inhibitory proteins, RASSF1 and NORE1, and by Ras. Biochem J 2004;381:453-62.

Richter AM, Pfeifer GP, Dammann RH. The RASSF proteins in cancer; from epigenetic silencing to functional characterization. Biochim Biophys Acta 2009;1796:114-28.

Rodriguez-Viciana P, Sabatier C, McCormick F. Signaling specificity by Ras family GTPases is determined by the full spectrum of effectors they regulate. Mol Cell Biol 2004;24:4943-54.

Scheel H, Hofmann K. A novel inter action motif, SARAH, connects three classes of tumor suppressor. Curr Biol 2003;13:R899-R900.

Stieglitz B, Bee C, Schwarz D, Yildiz O, Moshnikova A, Khokhlatchev A, et al. Novel type of Ras effector interaction established between tumour suppressor NORE1A and Ras switch II. EMBO J 2008;27:1995-2005.

Takahashi S, Ebihara A, Kajiho H, Kontani K, Nishina H, Katada T. RASSF7 negatively regulates pro-apoptotic JNK signaling by inhibiting the activity of phosphorylated-MKK7. Cell Death Differ 2011;18:645-55.

Vos MD, Ellis CA, Bell A, Birrer MJ, Clark GJ. Ras uses the novel tumor suppressor RASSF1 as an effector to mediate apoptosis. J Biol Chem 2000;275:35669-72.

Vos MD, Ellis CA, Elam C, Ulku AS, Taylor BJ, Clark GJ. RASSF2 is a novel K-Ras-specific effector and potential tumor suppressor. J Biol Chem 2003a;278:28045-51.

Vos MD, Martinez A, Ellis CA, Vallecorsa T, Clark GJ. The pro-apoptotic Ras effector Nore1 may serve as a Ras-regulated tumor suppressor in the lung. J Biol Chem 2003b;278:21938-43.

Xu D, Zhang Y. Ab initio protein structure assembly using continuous structure fragments and optimized knowledge-based force field. Proteins 2012;80:1715-35.

Figure Legends

Figure 1 Schematic representation of the RASSF family

There are many splice variants of the RASSF members. The most common one has been selected for each member and two for RASSF5: RASSF5A and RASSF5C, also known as RAPL. The classical RASSF1-6 are on the left and the N-terminal RASSF7-10 on the right. Characteristic domains shown are the Protein Kinase C conserved region, C1 (grey), the Ras-association domain, RA (green), the Sav-RASSF-Hpo domain, SARAH (blue) and the coiled-coil regions (orange).

Figure 2 Modelling the RASSF RA domain and predicting its interactions

(A) Multiple sequence alignment of the RA domain of RASSF1-6 predicted by Prosite. Secondary structural elements are indicated above. The residues in RASSF5 involved in electrostatic interactions with Ras are marked with an asterisk (*) above and the conserved residues aligning to those positions are highlighted in grey. Other residues are coloured according to their similarity, fully conserved residues in red, highly similar residues in green and weakly similar residues in blue.

(B) Ribbon representations show the classical RASSF RA domain modelled against RASSF5 (PDB: 3DDC). Side chains of the conserved residues aligning to those in RASSF5 involved in electrostatic interactions are in pink and labelled. The surface electrostatic potential is superimposed; positively charged regions are in blue and negatively charged regions in red.

(C) Multiple sequence alignment of the RA domain of the N-terminal RASSF7-9 and c-Raf RBD. Secondary structural elements and conserved residues are labelled and highlighted as in (A).

(D) Ribbon representations show the N-terminal RASSF7-9 RA domain modelled against c-Raf RBD (PDB: 1GUA) are presented and labelled as in (B).

Figure 3 RA domain of RASSF1-10 shows differential Ras interactions

Pull-down analysis of GFP-RASSF1-10 in cell lysates binding to immobilised activated HRas G12V loaded with GDP (D) or GTP (T). The lower panels are Ras and RASSF loading controls, and the GAPDH endogenous control.

Figure 4 Modelling the RASSF SARAH domain and predicting its interactions

(A) Multiple sequence alignment of the SARAH domain of MST1 kinase and RASSF1-6. The secondary structural elements are indicated as helix 1 (H1) and helix 2 (H2). Residues in MST1 involved in electrostatic interactions are marked with an arrow head (^), hydrophobic interactions for monomer stability with a dot (.) and for dimer stability with an asterisk (*). Conserved residues aligning to the positions marked with . or * are highlighted in grey. Residues in red are fully conserved, green highly similar and blue weakly similar.

(B) Ribbon representations show the classical RASSF SARAH domains modelled against MST1 kinase (PDB: 2JO8). Basic residues are in blue, acidic in red, polar in white and hydrophobic in yellow. Side chains of hydrophobic residues involved in dimer stability are shown in yellow and labelled.

Figure 5 SARAH domain mediates dimerisation between RASSF and MST kinases

(A) Co-IP analysis of GFP-RASSF5 interacting with myc-MST1, myc-MST2 or their kinase-dead mutants K59R and K56R respectively. Anti-myc antibody was used to immunoprecipitate (IP) MST and their interaction with GFP-RASSF5 was detected by immunoblotting (IB).

(B) Co-IP analysis of wild-type (WT) GFP-RASSF5 or RASSF5 SARAH domain deletion (Δ213-265) and myc-MST mutants is on the left. The RASSF5 loading control and GAPDH endogenous control are on the right.

(C) Co-IP analysis of GFP-RASSF1-10 interacting with myc-MST1 K59R (left) or myc-MST2 K56R (right). The RASSF and MST loading controls and GAPDH endogenous control are shown below the co-IP panels for each set of cell lysates.

(D) Analysis of RASSF7 interaction with MST. (a) Co-IP analysis of GFP-RASSF5 or RASSF7 and myc-MST1 K59R. A simultaneous negative control was performed without the anti-myc antibody. The RASSF loading control and GAPDH endogenous control are on the right. (b) 3D models of the two coiled-coil regions of RASSF7 predicted by Prosite. The residues are labelled as in Fig. 3B and side chains of hydrophobic residues on the same face of the helix are shown in yellow.

Figure 6 Schematic model of interaction between the RASSF family and MST kinases

The Ras GTPase family is shown as cyan boxes that bind to the RA domain of different RASSF members represented by the ubiquitin-fold ribbon structure in blue and yellow. The SARAH domains are shown as anti-parallel helices from different RASSF members or MST kinase, in purple and green. The ability of the SARAH domain to mediate protein-protein interactions could be a basis for the formation of (A) homodimers between two different RASSF members or (B) heterodimers between RASSF members and other SARAH domain-containing proteins such as MST kinases. These interactions could be regulated by Ras interaction with the RA domain.

Supplementary Data

Supplementary Figure 1 3D models of RASSF5 RA and c-Raf RBD

(A) The ribbon representation of RASSF5 RA domain (residues 274-357) is derived from the PDB structure 3DDC. Residues involved in electrostatic interactions with Ras are highlighted in pink and labelled. The surface electrostatic potential is superimposed on the model with positively charged regions in blue and negatively charged regions in red.

(B) The ribbon representation of c-Raf RBD (PDB: 1GUA). Residues involved in electrostatic interactions with Ras are in yellow and labelled. The surface electrostatic potential is shown as in (A).

(C) The ribbon representation of the MST1 kinase SARAH domain (PDB: 2JO8). Basic residues are in blue, acidic in red, polar in white and hydrophobic in yellow. Side chains of the hydrophobic residues involved in dimer stability are shown in yellow and labelled.

Supplementary Figure 2 Analysis of the interaction between isolated SARAH domains

(A) Pull-down analysis of purified protein of MST1 SARAHmyc binding to immobilised S-RASSF5 SARAH.

(B) Mass spectra of MST1 SARAHmyc and RASSF5 SARAH proteins under native MS conditions. From top to bottom: mass spectrum of MST1 SARAHmyc, RASSF5 SARAH and MST1 SARAHmyc mixed with RASSF5 SARAH. Charge states corresponding to MST1 SARAHmyc monomer, dimer, and RASSF5 SARAH monomer and dimer, are indicated and coloured in red and blue, green and cyan, respectively. The table below compares the protein monomeric and dimeric mass measurements to the theoretical masses. The low error confirms the accuracy of the experimental results.

(C) Co-IP analysis of TagRFPT-MST1 SARAH and myc-RASSF5 SARAH, in which full length (FL) MST1 served as a positive control.

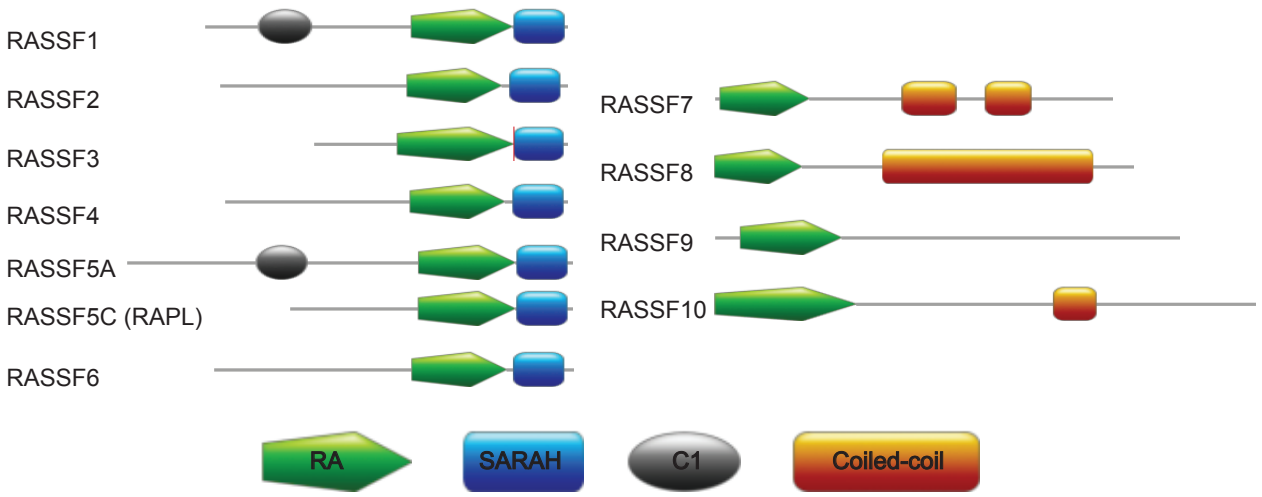
RASSF1
RASSF2
RASSF3
RASSF4
RASSF5A
RASSF5C (RAPL)
RASSF6
RASSF7
RASSF8
RASSF9
RASSF10
RA
SARAH
C1
Coiled-coil

Figure 1

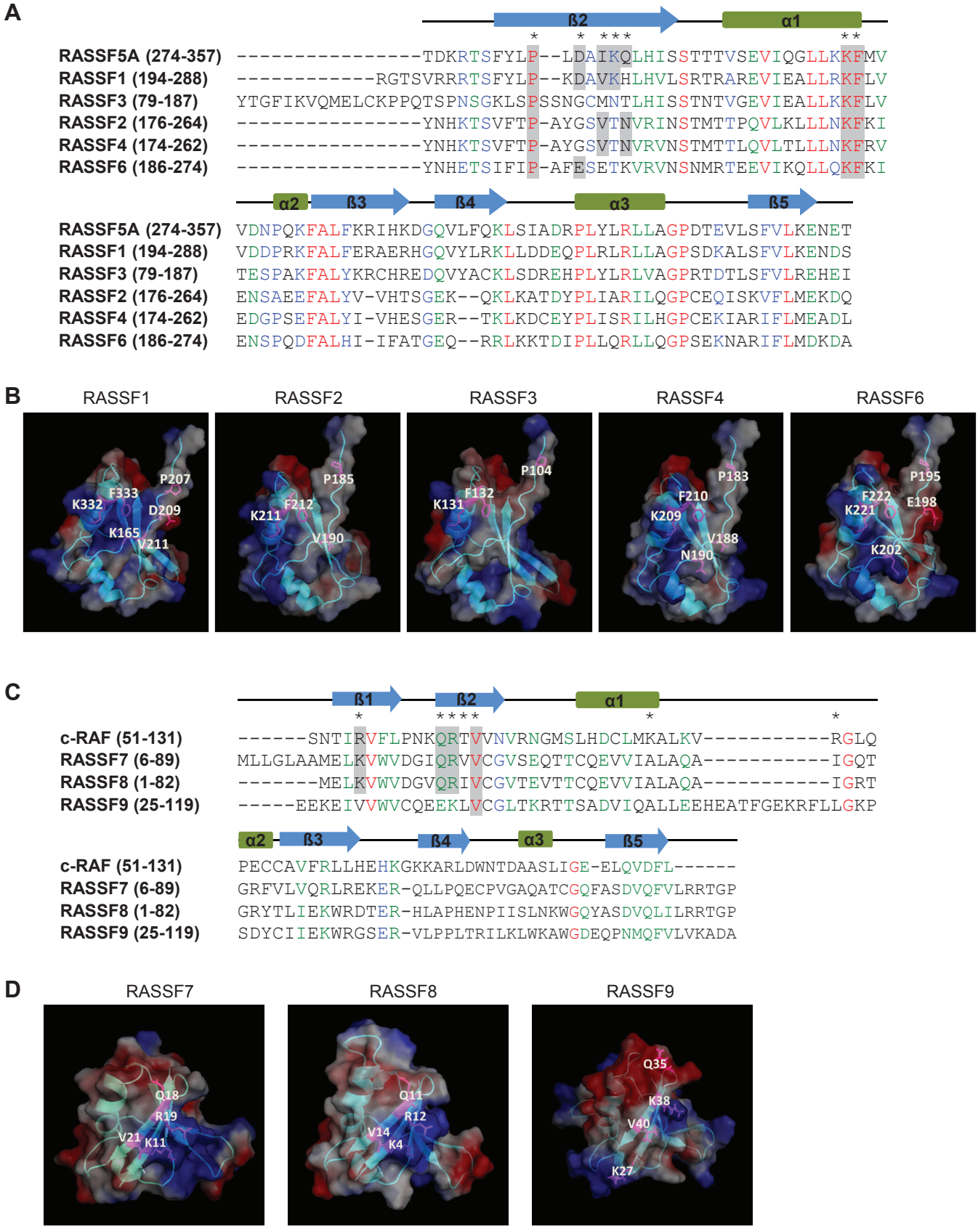
A
ß2
α1
RASSF5A (274-357) ----------TDKRTSFYLP--LDAIKQLHISSTTTVSEVIQGLLKKFMV
RASSF1 (194-288) ----------RGTSVRRRTSFYLP--KDAVKHLHVLSRTRAREVIEALLRKFLV
RASSF3 (79-187) YTGFIKVQMELCKPPQTSPNSGKLSPSSNGCMNTLHISSTNTVGEVIEALLKKFLV
RASSF2 (176-264) ----------YNHKTSVFTP-AYGSVTNVRINSTMTTPQVLKLLLNKFKI
RASSF4 (174-262) ----------YNHKTSVFTP-AYGSVTNVRVNSTMTTLQVLTLLLNKFRV
RASSF6 (186-274) ----------YNHETSIFIP-AFESETKVRVNSNMRTEEVIKQLLQKFKI
α2
ß3
ß4
α3
ß5
RASSF5A (274-357) VDNPQKFALFKRIHKDGQVLFQKLSIADRPLYLRLLAGPDTEVLSFVLKENET
RASSF1 (194-288) VDDPRKFALFERAERHGQVYLRKLLDDEQPLRLRLLAGPSDKALSFVLKENDS
RASSF3 (79-187) TESPAKFALYKRCHREDQVYACKLSDREHPLYLRLVAGPRTDTLSFVLREHEI
RASSF2 (176-264) ENSAEEFALYV-VHTSGEK--QKLKATDYPLIARILQGPCEQISKVFLMEKDQ
RASSF4 (174-262) EDGPSEFALYI-VHESGER--TKLKDCEYPLISRILHGPCEKIARIFLMEADL
RASSF6 (186-274) ENSPQDFALHI-IFATGEQ--RRLKKTDIPLLQRLLQGPSEKNARIFLMDKDA
B
RASSF1
RASSF2
RASSF3
RASSF4
RASSF6
P207
F333
K332
D209
K165
V211
P185
F212
K211
V190
P104
F132
K131
P183
F210
K209
V188
N190
P195
F222
K221
E198
K202
C
ß1
ß2
α1
c-RAF (51-131) ------SNTIRVFLPNKQRTVVNVRNGMSLHDCLMKALKV----------RGLQ
RASSF7 (6-89) MLLGLAAMELKVWVDGIQRVVCGVSEQTTCQEVVIALAQA----------IGQT
RASSF8 (1-82) -------MELKVWVDGVQRIVCGVTEVTTCQEVVIALAQA----------IGRT
RASSF9 (25-119) -----EEKEIVVWVCQEEKLVCGLTKRTTSADVIQALLEEHEATFGEKRFLLGKP
α2
ß3
ß4
α3
ß5
c-RAF (51-131) PECCAVFRLLHEHKGKKARLDWNTDAASLIGE-ELQVDFL------
RASSF7 (6-89) GRFVLVQRLREKER-QLLPQECPVGAQATCGQFASDVQFVLRRTGP
RASSF8 (1-82) GRYTLIEKWRDTER-HLAPHENPIISLNKWGQYASDVQLILRRTGP
RASSF9 (25-119) SDYCIIEKWRGSER-VLPPLTRILKLWKAWGDEQPNMQFVLVKADA
D
RASSF7
RASSF8
RASSF9
Q18
R19
V21
K11
Q11
R12
V14
K4
Q35
K38
V40
K27

Figure 2

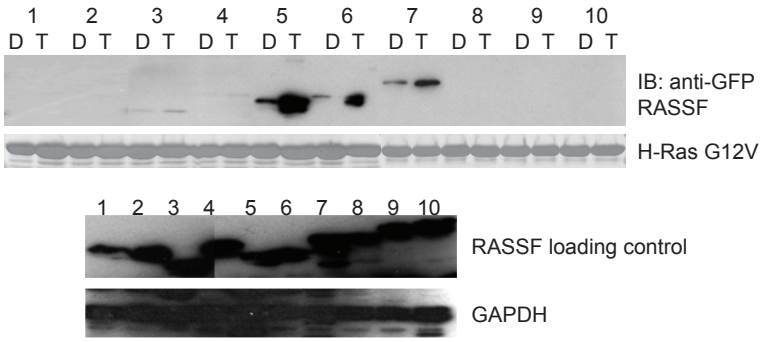
1 2 3 4 5 6 7 8 9 10
D T D T D T D T D T D T D T D T D T D T
IB: anti-GFP
RASSF
H-Ras G12V

1 2 3 4 5 6 7 8 9 10
RASSF loading control
GAPDH

Figure 3

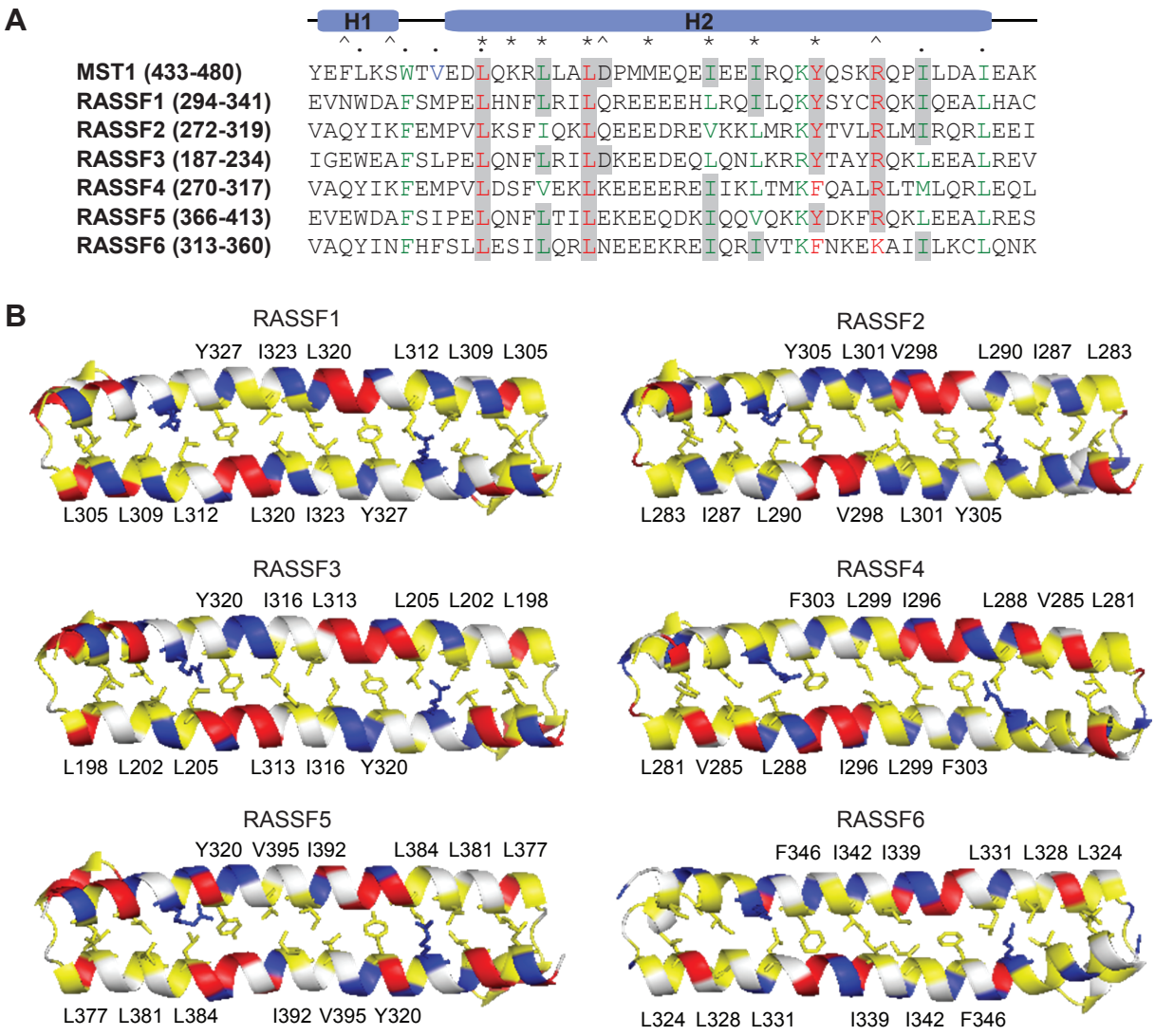
A
H1
H2
MST1 (433-480) YEFLKSWTVEDLQKRLLALDPMMEQEIEEIRQKYQSKRQPILDAIEAK
RASSF1 (294-341) EVNWDAFSMPELHNFLRILQREEEEHLRQILQKYSYCRQKIQEALHAC
RASSF2 (272-319) VAQYIKFEMPVLKSFIQKLQEEEDREVKKLMRKYTVLRLMIRQRLEEI
RASSF3 (187-234) IGEWEAFSLPELQNFLRILDKEEDEQLQNLKRRYTAYRQKLEEALREV
RASSF4 (270-317) VAQYIKFEMPVLDSFVEKLKEEEEREIIKLTMKFQALRLTMLQRLEQL
RASSF5 (366-413) EVEWDAFSIPELQNFLTILEKEEQDKIQQVQKKYDKFRQKLEEALRES
RASSF6 (313-360) VAQYINFHFSLLESILQRLNEEEKREIQRIVTKFNKEKAIILKCLQNK
B
RASSF1
Y327 I323 L320 L312 L309 L305
L305 L309 L312 L320 I323 Y327
RASSF2
Y305 L301 V298 L290 I287 L283
L283 I287 L290 V298 L301 Y305
RASSF3
Y320 I316 L313 L205 L202 L198
L198 L202 L205 L313 I316 Y320
RASSF4
F303 L299 I296 L288 V285 L281
L281 V285 L288 I296 L299 F303
RASSF5
Y320 V395 I392 L384 L381 L377
L377 L381 L384 I392 V395 Y320
RASSF6
F346 I342 I339 L331 L328 L324
L324 L328 L331 I339 I342 F346

Figure 4

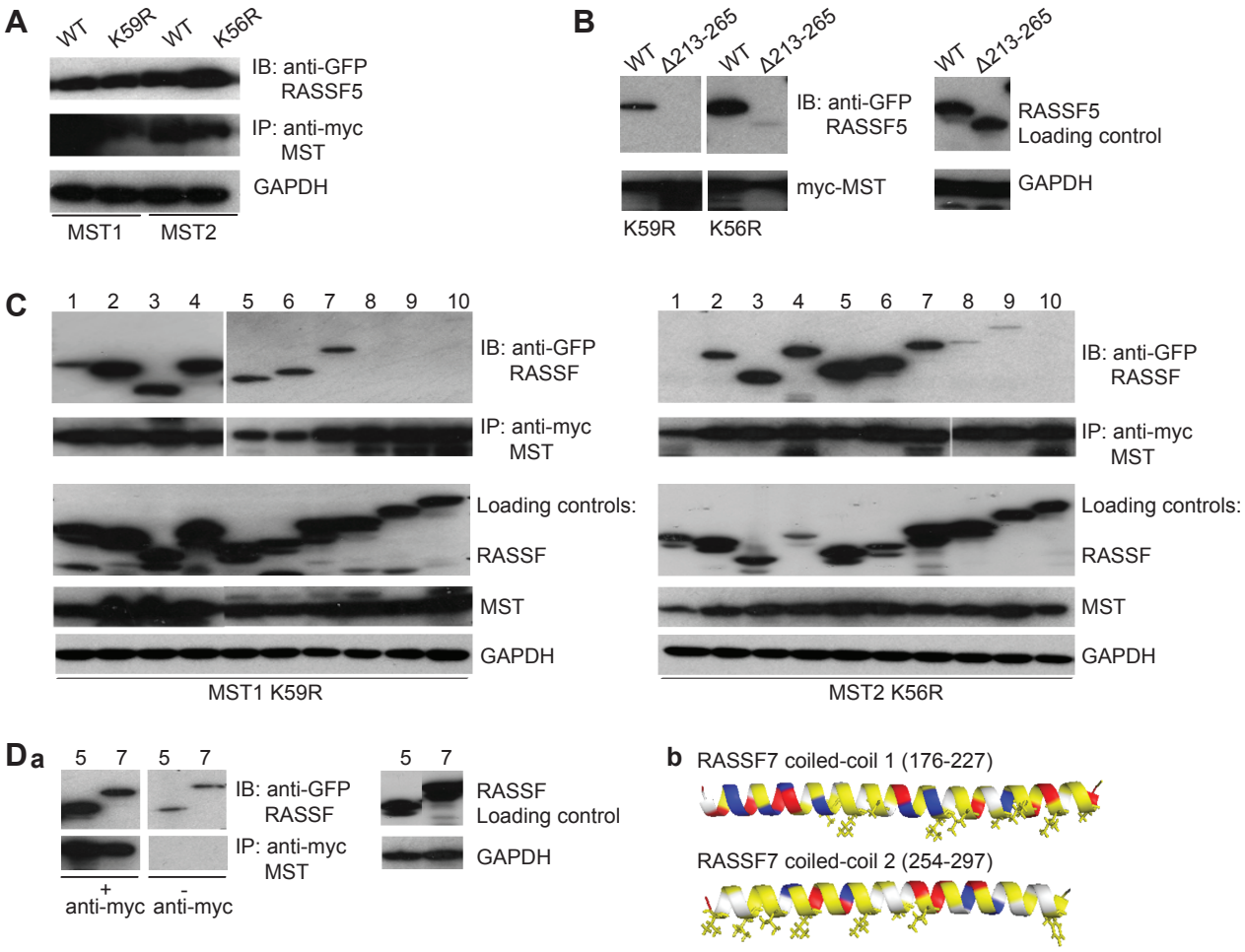
A
WT
K59R
WT
K56R
IB: anti-GFP
RASSF5
IP: anti-myc
MST
GAPDH
MST1
MST2
B
WT
Δ213-265
WT
Δ213-265
IB: anti-GFP
RASSF5
myc-MST
K59R
K56R
WT
Δ213-265
RASSF5
Loading control
GAPDH
C
1 2 3 4 5 6 7 8 9 10
IB: anti-GFP
RASSF
IP: anti-myc
MST
Loading controls:
RASSF
MST
GAPDH
MST1 K59R
1 2 3 4 5 6 7 8 9 10
IB: anti-GFP
RASSF
IP: anti-myc
MST
Loading controls:
RASSF
MST
GAPDH
MST2 K56R
Da
5 7
5 7
IB: anti-GFP
RASSF
IP: anti-myc
MST
+
anti-myc
-
anti-myc
5 7
RASSF
Loading control
GAPDH
b
RASSF7 coiled-coil 1 (176-227)
RASSF7 coiled-coil 2 (254-297)

Figure 5

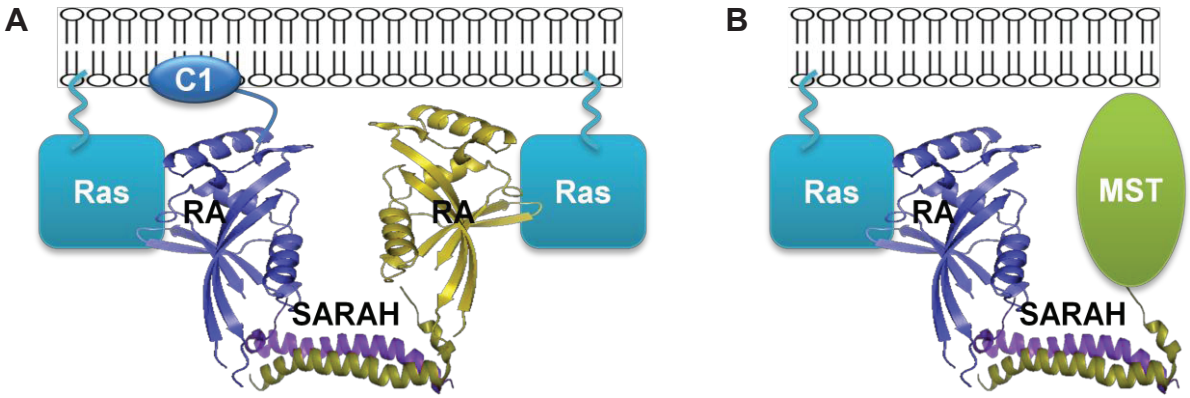

Figure 6

Supplementary Figure 1

A

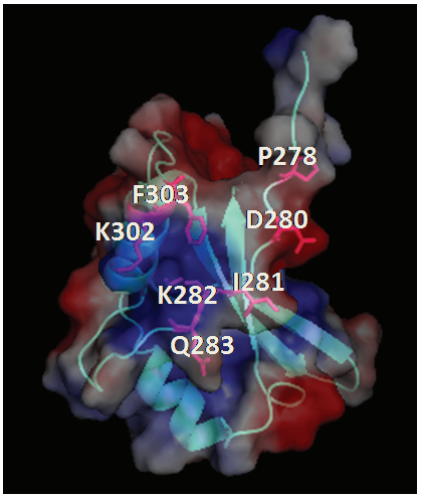

B

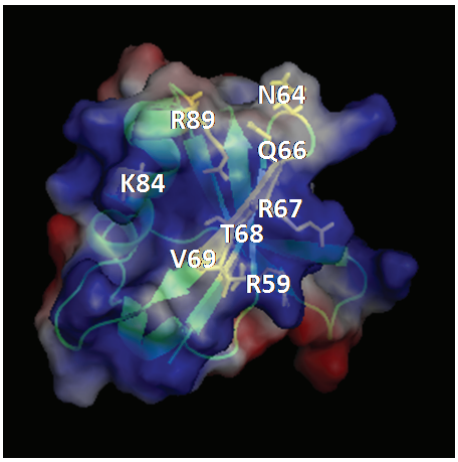

C

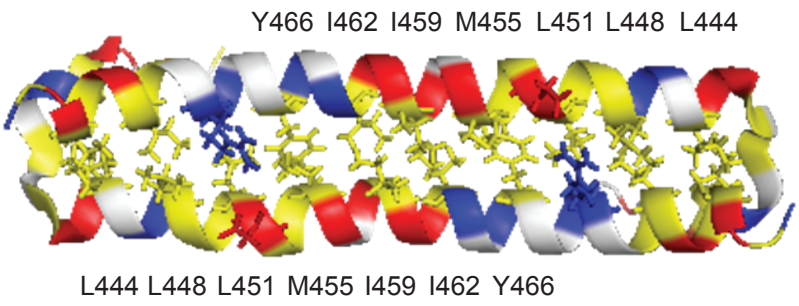

Supplementary Figure 2

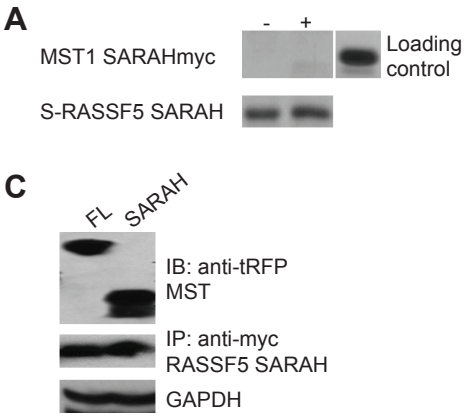

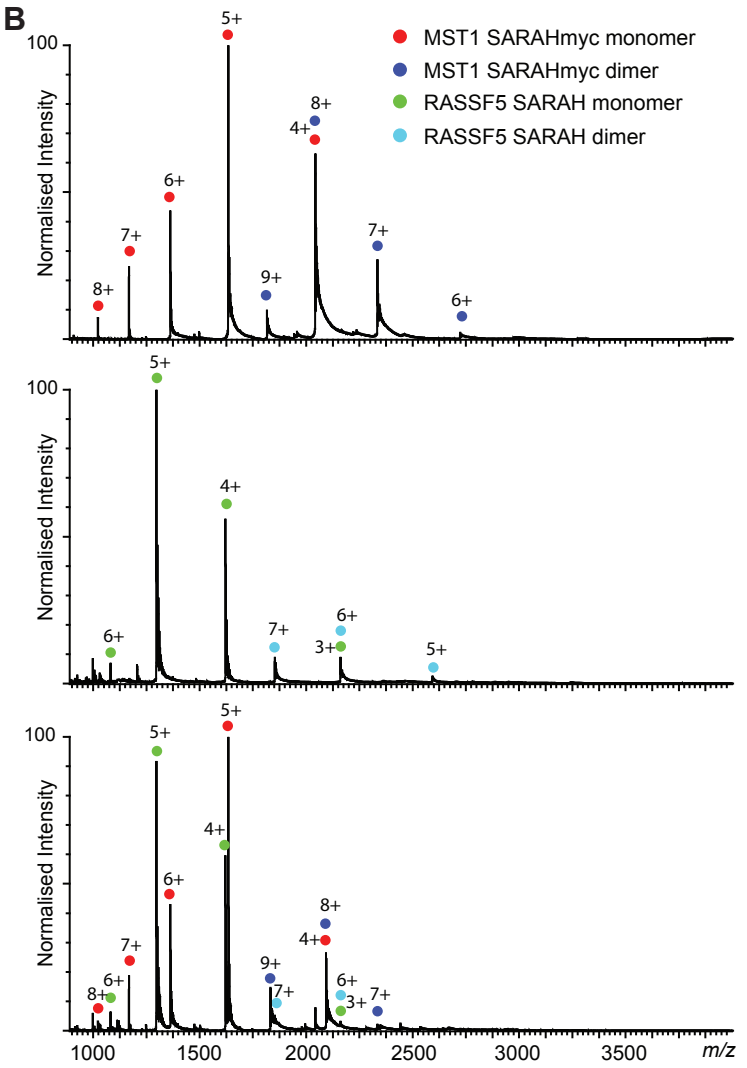

	Experimental Mass	Theoretical Mass
MST1 SARAHmyc monomer	8167.9 ± 0.1 Da	8168.3 Da
MST1 SARAHmyc dimer	16336.7 ± 0.1 Da	16336.6 Da
RASSF5 SARAH monomer	6479.9 ± 0.1 Da	6480.3 Da
RASSF5 SARAH dimer	12961.4 ± 0.2 Da	12960.6 Da